

# Gender classification via functional connectivity

GUO Siye LIU Chang WANG Zeyu ZHANG Qidan

November 13, 2024

# Contents

1 Introduction

2 Materials and methods

3 Analysis

4 Discussion

# Introduction

The previous work shows that there exists gender differences for structure connectivity or brain image<sup>[1][2][3]</sup>:

- Women showed greater overall cortical connectivity and the underlying organization of their cortical networks was more efficient compared with men;
- Gender differences may be reflected in anatomical structures.

Some research on disease also report the gender effect<sup>[4]</sup> or regard the gender as potential confounding effects<sup>[5]</sup>.

---

<sup>[1]</sup> Gaolang Gong et al. (2009). "Age- and gender-related differences in the cortical anatomical network". en. In: *J. Neurosci.* 29, 50, pp. 15684–15693.

<sup>[2]</sup> Mahsa Dibaji et al. (2023). "Studying the effects of sex-related differences on brain age prediction using brain MR imaging". In: *Clinical Image-Based Procedures, Fairness of AI in Medical Imaging, and Ethical and Philosophical Issues in Medical Imaging*. Cham: Springer Nature Switzerland, pp. 205–214.

<sup>[3]</sup> Matthias Ebel et al. (2023). "Classifying sex with volume-matched brain MRI". en. In: *NeuroImage Rep.* 3, 3, p. 100181.

<sup>[4]</sup> Mohammad S E Sendi et al. (2023). "The link between static and dynamic brain functional network connectivity and genetic risk of Alzheimer's disease". en. In: *NeuroImage Clin.* 37, 103363, p. 103363.

<sup>[5]</sup> Weizheng Yan et al. (2019). "Discriminating schizophrenia using recurrent neural network applied on time courses of multi-site fMRI data". en. In: *EBioMedicine* 47, pp. 543–552.

# Introduction

Model	Result
SVM <sup>[6]</sup>	across sample AUC: 0.718( $\pm 0.2$ ) within sample AUC: 0.716( $\pm 0.156$ )
CNN <sup>[7]</sup>	rsfMRI AUC: 0.8923 tfMRI AUC: 0.7683
SVM <sup>[8]</sup>	avg ACC: 0.687 max ACC: 0.751
Partial least squares regression <sup>[9]</sup>	AUC: 0.93, ACC: 0.85

**Table:** The models and results of previous papers using static functional connectivity (sFC).

<sup>[6]</sup>Obada Al Zoubi et al. (2020). "Predicting sex from resting-state fMRI across multiple independent acquired datasets".

<sup>[7]</sup>Matthew Leming and John Suckling (2021). "Deep learning for sex classification in resting-state and task functional brain networks from the UK Biobank". en. In: *Neuroimage* 241.118409, p. 118409.

<sup>[8]</sup>Susanne Weis et al. (2020). "Sex classification by resting state brain connectivity". en. In: *Cereb. Cortex* 30.2, pp. 824–835.

<sup>[9]</sup>Chao Zhang et al. (2018). "Functional connectivity predicts gender: Evidence for gender differences in resting brain connectivity". en. In: *Hum. Brain Mapp.* 39.4, pp. 1765–1776.

# Introduction

Model	Result
CNN and LSTM <sup>[10]</sup>	AUC: 0.9805, ACC: 0.9305( $\pm 0.0191$ )
Statistic analysis <sup>[11]</sup>	Pearson dFC: ACC: 0.7984 Partial sFC: ACC: 0.9005 Pearson sFC: ACC: 0.6839
Random forest <sup>[12]</sup>	ACC: 0.94

**Table:** The models and results of previous papers using dynamic functional connectivity (dFC).

---

[10] Liangwei Fan et al. (2020). "A deep network model on dynamic functional connectivity with applications to gender classification and intelligence prediction". en. In: *Front. Neurosci.* 14, p. 881.

[11] Sreevalsan S Menon and K Krishnamurthy (2019). "A comparison of static and dynamic functional connectivities for identifying subjects and biological sex using intrinsic individual brain connectivity". en. In: *Sci. Rep.* 9.1, p. 5729.

[12] Bhaskar Sen and Keshab K Parhi (2021). "Predicting biological gender and intelligence from fMRI via dynamic functional connectivity". en. In: *IEEE Trans. Biomed. Eng.* 68.3, pp. 815–825.

## HCP dataset<sup>[13][14]</sup>

- Originates from brain data of more than 1000 healthy adults;
- Collects a large amount of neuroimaging data that reflects the functional connectivity of the human brain;
- Covers a variety of experimental conditions, including task state, resting state, etc;
- Widely used in various neuroscience studies, such as psychiatric studies.

---

<sup>[13]</sup> Matthew F Glasser et al. (2013). "The minimal preprocessing pipelines for the Human Connectome Project". en. In: *Neuroimage* 80, pp. 105–124.

<sup>[14]</sup> D C Van Essen et al. (2012). "The Human Connectome Project: a data acquisition perspective". en. In: *Neuroimage* 62.4, pp. 2222–2231.

# Preprocessing

The following is one of the most commonly used preprocessing method<sup>[15][16][17][18]</sup> (and also used by HCP dataset):

- Pre-process fMRI image data including spatial normalization, noise reduction, etc;
- Use group-ICA to decompose the brain regions;
- For each brain region, compute the representative timeseries;
- Compute the functional connectivity via partial correlation.

For the dynamic functional connectivity, we apply the sliding window method<sup>[19]</sup> and compute the partial correlation in each window.

---

[15] N Filippini et al. (2009). "Distinct patterns of brain activity in young carriers of the APOE-e4 allele". In: *Proc Natl Acad Sci* 106, pp. 7209–7214.

[16] Christian F Beckmann and Stephen M Smith (2004). "Probabilistic independent component analysis for functional magnetic resonance imaging". en. In: *IEEE Trans. Med. Imaging* 23.2, pp. 137–152.

[17] Stephen M Smith et al. (2011). "Network modelling methods for fMRI". en. In: *Neuroimage* 54.2, pp. 875–891.

[18] Stephen M Smith et al. (2013). "Functional connectomics from resting-state fMRI". en. In: *Trends Cogn. Sci.* 17.12, pp. 666–682.

[19] Elena A Allen et al. (2014). "Tracking whole-brain connectivity dynamics in the resting state". en. In: *Cereb. Cortex* 24.3, pp. 663–676.

# Preprocessing - Examples

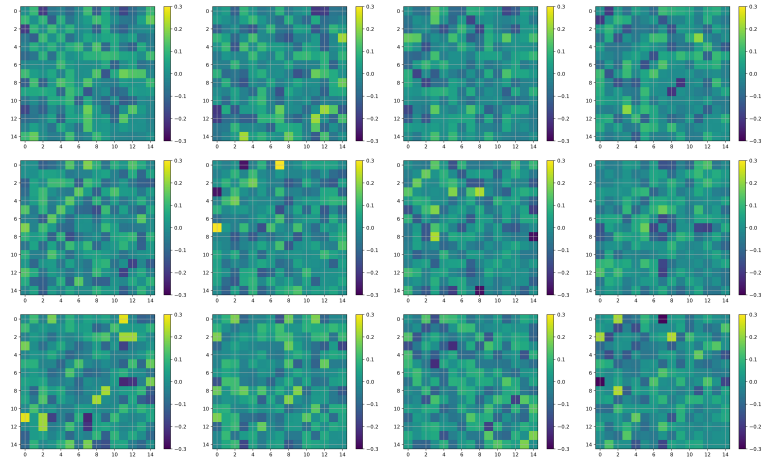


Figure: Centered dynamic functional connectivity with  $N_{node} = 15$ .

# Preprocessing - Examples

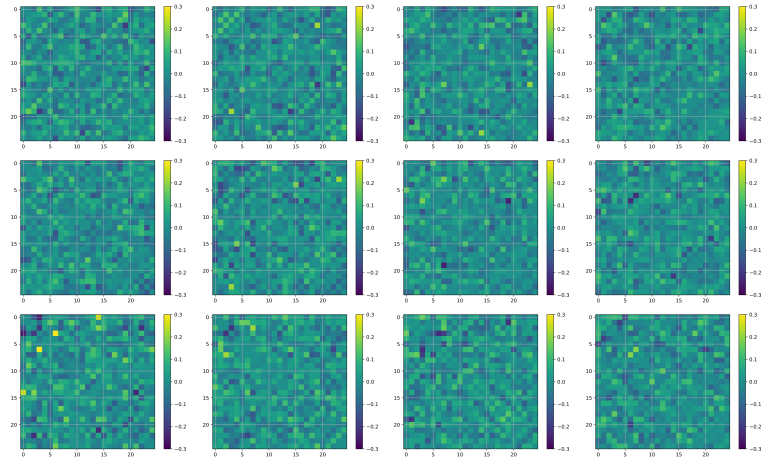


Figure: Centered dynamic functional connectivity with  $N_{node} = 25$ .

# Preprocessing - Examples

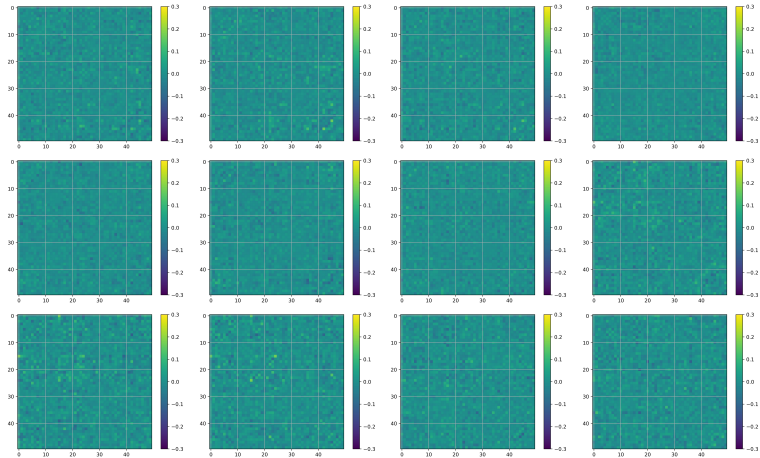


Figure: Centered dynamic functional connectivity with  $N_{node} = 50$ .

## Preprocessing - Examples

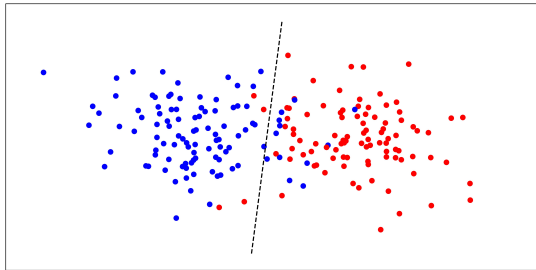
We compute the variance of each entry in dFC, which shows that the frames of dFC are more uniform with the increase of node.

$N_{node}$	min	mean	max
15	5.76e-6	2.80e-5	1.99e-4
25	2.82e-6	1.07e-5	6.07e-5
50	1.63e-8	1.34e-6	4.90e-6

Table: Variance of dFC

# SVM<sup>[20][21]</sup>

Given a dataset  $\{(\mathbf{x}_i, y_i)\}_{i=1}^N$ , a linear SVM aims to find a vector  $\mathbf{w}$  and a number  $b$  such that the data can be separated via the distance  $\mathbf{w}^T \mathbf{x}_i - b$ .



[20] Vladimir N Vapnik (1997). "The support vector method". In: *Lecture Notes in Computer Science*. Berlin, Heidelberg: Springer Berlin Heidelberg, pp. 261–271.

[21] Corinna Cortes and Vladimir Vapnik (1995). "Support-vector networks". en. In: *Mach. Learn.* 20.3, pp. 273–297.

# SVM - Results

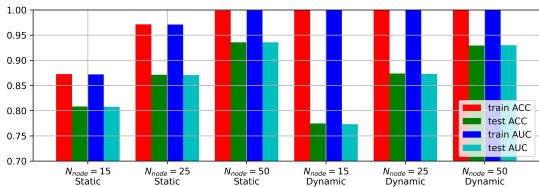


Figure: Results of Linear SVM.

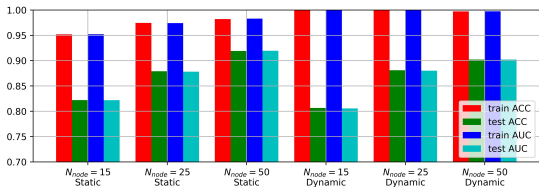
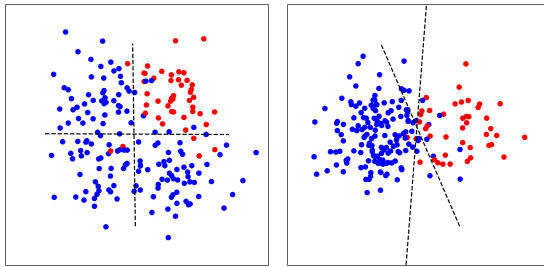


Figure: Results of Nu-SVM.

## CNN - Model

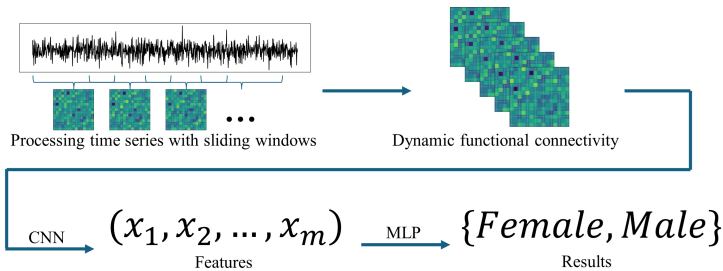
Given a dataset  $\{(\mathbf{x}_i, y_i)\}_{i=1}^N$ , we aim to find some vectors  $\{\mathbf{w}_k\}_{k=1}^m$  and some numbers  $\{b_k\}_{k=1}^m$  such that any given data  $\mathbf{x}$  can be classified via the tuple of distance  $(\mathbf{w}_1^T \mathbf{x} - b_1, \dots, \mathbf{w}_m^T \mathbf{x} - b_m)$ .

In the worst case, all the  $\mathbf{w}_k$  and  $b_k$  are the same, then the results should be the same with linear SVM.



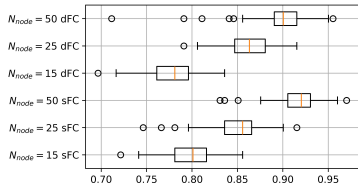
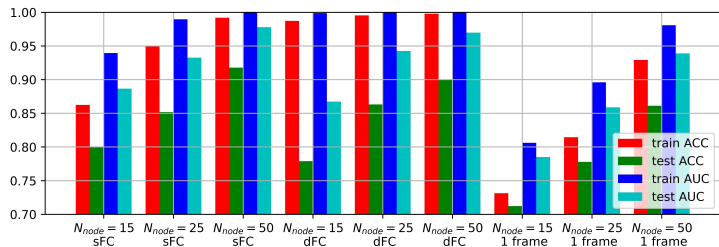
# CNN - Model

The followings are the flowchart of our method, where we use a 1-layer 1-dimensional CNN with size equivalent to the input shape, so that it is the same as previous statements.

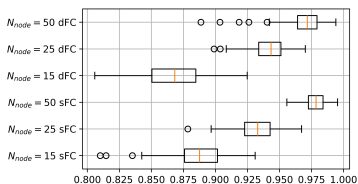


We split the data into training dataset (80%) and test dataset (20%), and repeat the experiment for 150 times to avoid flukes.

# CNN - Results



(a) test ACC



(b) test AUC

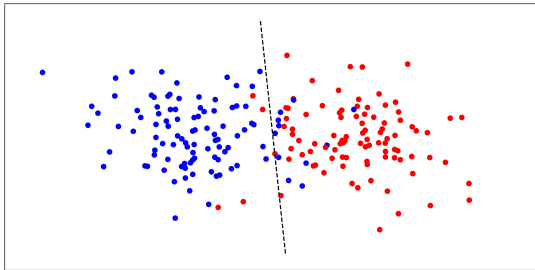
Figure: Results of CNN model with dropout = 0.1 and channel = 4.

# CNN - Results

- More nodes leads to a higher accuracy and AUC;
- The choice of sFC and dFC will not significantly affect the result;
- The accuracy rate will decrease when using the sub-series.

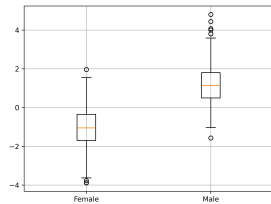
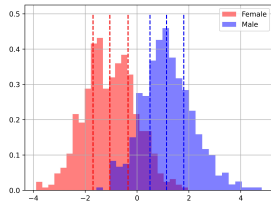
## LDA<sup>[22]</sup>

Given a dataset  $\{\mathbf{x}_i, y_i\}_{i=1}^N$ , the LDA aims to find a vector pair  $\mathbf{y}, \mathbf{c}$  such that the inner product  $\langle \mathbf{x}_i - \mathbf{c}, \mathbf{y} \rangle$  minimizes the interclass variance and maximizes the distance between the projected means of the classes.

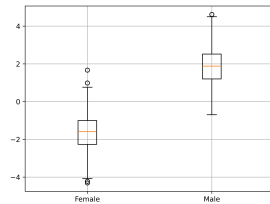
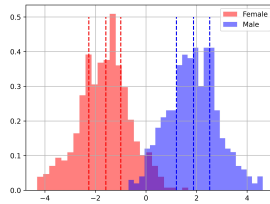


<sup>[22]</sup>Harvey Goldstein, Jacob Cohen, and Patricia Cohen (1976). "Applied multiple regression/correlation analysis for the behavioural sciences". In: *J. R. Stat. Soc. Ser. A* 139.4, p. 549.

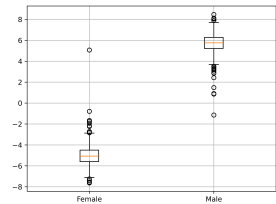
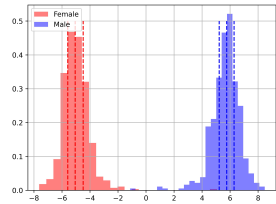
# LDA - sFC



(a)  $N_{node} = 15$



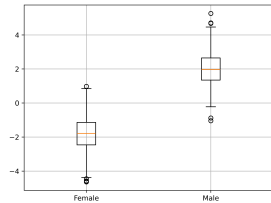
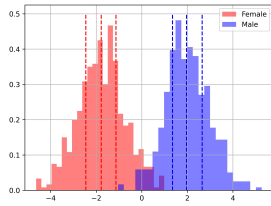
(b)  $N_{node} = 25$



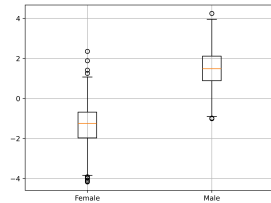
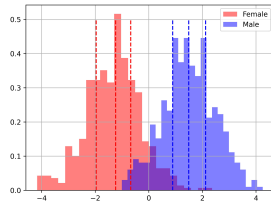
(c)  $N_{node} = 50$

Figure: LDA for sFC.

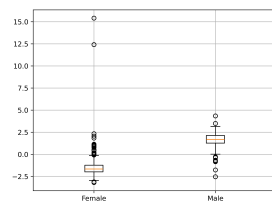
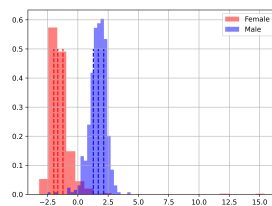
# LDA - dFC



(a)  $N_{node} = 15$



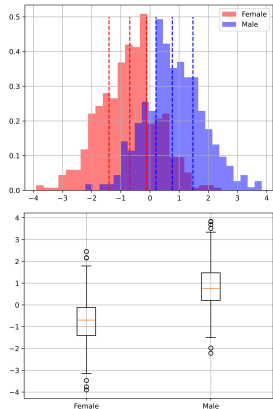
(b)  $N_{node} = 25$



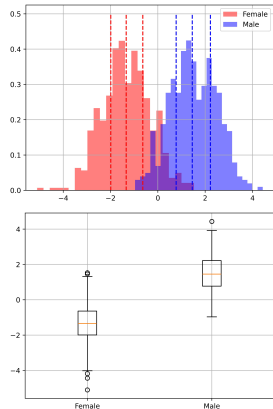
(c)  $N_{node} = 50$

Figure: LDA for dFC.

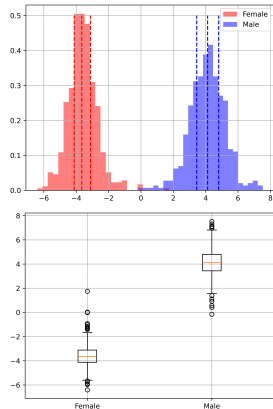
# LDA - dFC



(a)  $N_{node} = 15$



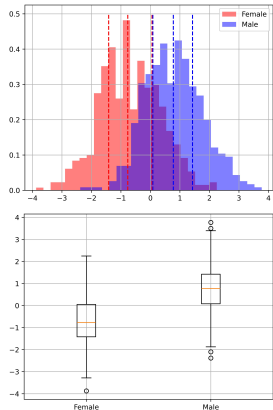
(b)  $N_{node} = 25$



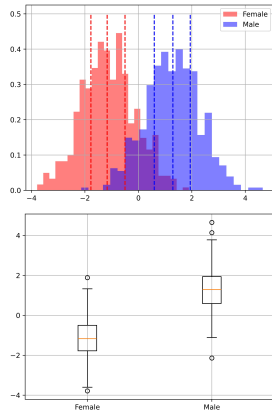
(c)  $N_{node} = 50$

Figure: LDA for 1-frame of dFC with max score.

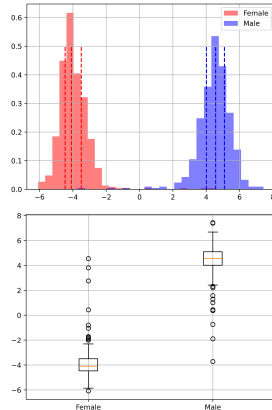
# LDA - dFC



(a)  $N_{node} = 15$



(b)  $N_{node} = 25$



(c)  $N_{node} = 50$

Figure: LDA for 1-frame of dFC with min score.

## LDA - Results

- Both sFC and dFC is linear separable;
- The overlap become less with the increase of node;
- The dFC is not always better than sFC, especially when there exists some outliers.

# Discussion

- Both sFC and dFC is linear separable;
- Both sFC and dFC can be used to predict gender with high accuracy and AUC;
- More nodes leads to a higher accuracy and AUC;
- The choice of sFC and dFC will not significantly affect the accuracy rate and AUC;
- The brain noise<sup>[23]</sup> will affect more on the dFC.

---

<sup>[23]</sup>spontaneous fluctuations in the electrical activity of the neurons

## Future research directions

- Choose a more reasonable size and step of the window via Fourier analysis, wavelet analysis, etc;
- Force the coefficient of CNN to be orthogonal;
- Use some simple nonlinear classifier (i.e. quadratic classifier).

# Reference I

-  Al Zoubi, Obada et al. (2020). "Predicting sex from resting-state fMRI across multiple independent acquired datasets".
-  Allen, Elena A et al. (2014). "Tracking whole-brain connectivity dynamics in the resting state". en. In: *Cereb. Cortex* 24.3, pp. 663–676.
-  Beckmann, Christian F and Stephen M Smith (2004). "Probabilistic independent component analysis for functional magnetic resonance imaging". en. In: *IEEE Trans. Med. Imaging* 23.2, pp. 137–152.
-  Cortes, Corinna and Vladimir Vapnik (1995). "Support-vector networks". en. In: *Mach. Learn.* 20.3, pp. 273–297.
-  Dibaji, Mahsa et al. (2023). "Studying the effects of sex-related differences on brain age prediction using brain MR imaging". In: *Clinical Image-Based Procedures, Fairness of AI in Medical Imaging, and Ethical and Philosophical Issues in Medical Imaging*. Cham: Springer Nature Switzerland, pp. 205–214.

## Reference II

-  Ebel, Matthis et al. (2023). "Classifying sex with volume-matched brain MRI". en. In: *Neuroimage Rep.* 3.3, p. 100181.
-  Fan, Liangwei et al. (2020). "A deep network model on dynamic functional connectivity with applications to gender classification and intelligence prediction". en. In: *Front. Neurosci.* 14, p. 881.
-  Filippini, N et al. (2009). "Distinct patterns of brain activity in young carriers of the APOE-e4 allele". In: *Proc Natl Acad Sci* 106, pp. 7209–7214.
-  Glasser, Matthew F et al. (2013). "The minimal preprocessing pipelines for the Human Connectome Project". en. In: *Neuroimage* 80, pp. 105–124.
-  Goldstein, Harvey, Jacob Cohen, and Patricia Cohen (1976). "Applied multiple regression/correlation analysis for the behavioural sciences". In: *J. R. Stat. Soc. Ser. A* 139.4, p. 549.

## Reference III

-  Gong, Gaolang et al. (2009). "Age- and gender-related differences in the cortical anatomical network". en. In: *J. Neurosci.* 29.50, pp. 15684–15693.
-  Leming, Matthew and John Suckling (2021). "Deep learning for sex classification in resting-state and task functional brain networks from the UK Biobank". en. In: *Neuroimage* 241.118409, p. 118409.
-  Menon, Sreevalsan S and K Krishnamurthy (2019). "A comparison of static and dynamic functional connectivities for identifying subjects and biological sex using intrinsic individual brain connectivity". en. In: *Sci. Rep.* 9.1, p. 5729.
-  Sen, Bhaskar and Keshab K Parhi (2021). "Predicting biological gender and intelligence from fMRI via dynamic functional connectivity". en. In: *IEEE Trans. Biomed. Eng.* 68.3, pp. 815–825.

## Reference IV

-  Sendi, Mohammad S E et al. (2023). "The link between static and dynamic brain functional network connectivity and genetic risk of Alzheimer's disease". en. In: *NeuroImage Clin.* 37.103363, p. 103363.
-  Smith, Stephen M et al. (2011). "Network modelling methods for fMRI". en. In: *Neuroimage* 54.2, pp. 875–891.
-  Smith, Stephen M et al. (2013). "Functional connectomics from resting-state fMRI". en. In: *Trends Cogn. Sci.* 17.12, pp. 666–682.
-  Van Essen, D C et al. (2012). "The Human Connectome Project: a data acquisition perspective". en. In: *Neuroimage* 62.4, pp. 2222–2231.
-  Vapnik, Vladimir N (1997). "The support vector method". In: *Lecture Notes in Computer Science*. Berlin, Heidelberg: Springer Berlin Heidelberg, pp. 261–271.
-  Weis, Susanne et al. (2020). "Sex classification by resting state brain connectivity". en. In: *Cereb. Cortex* 30.2, pp. 824–835.

## Reference V

-  Yan, Weizheng et al. (2019). "Discriminating schizophrenia using recurrent neural network applied on time courses of multi-site fMRI data". en. In: *EBioMedicine* 47, pp. 543–552.
-  Zhang, Chao et al. (2018). "Functional connectivity predicts gender: Evidence for gender differences in resting brain connectivity". en. In: *Hum. Brain Mapp.* 39.4, pp. 1765–1776.

## Ablation study

Data	Dropout	Channel	train ACC/AUC	test ACC/AUC
sFC	0.0	1	0.8605/0.9230	0.7892/0.8804
sFC	0.0	2	0.8837/0.9459	0.7972/0.8847
sFC	0.0	4	0.9070/0.9644	0.7956/0.8820
sFC	0.1	1	0.7975/0.8609	0.7971/0.8874
sFC	0.1	2	0.8217/0.9054	0.7975/0.8871
sFC	0.1	4	0.8624/0.9395	0.7993/0.8867
dFC	0.0	1	0.9719/0.9830	0.7755/0.8665
dFC	0.0	2	0.9952/0.9977	0.7791/0.8586
dFC	0.0	4	0.9990/0.9997	0.7783/0.8565
dFC	0.1	1	0.9224/0.9650	0.7773/0.8668
dFC	0.1	2	0.9715/0.9933	0.7778/0.8682
dFC	0.1	4	0.9873/0.9988	0.7790/0.8674

Table: Ablation study for  $N_{node} = 15$ .

## Ablation study

Data	Dropout	Channel	train ACC/AUC	test ACC/AUC
sFC	0.0	1	0.9539/0.9747	0.8400/0.9220
sFC	0.0	2	0.9913/0.9950	0.8472/0.9230
sFC	0.0	4	0.9959/0.9992	0.8461/0.9207
sFC	0.1	1	0.8760/0.9274	0.8429/0.9277
sFC	0.1	2	0.9202/0.9751	0.8550/0.9334
sFC	0.1	4	0.9507/0.9897	0.8518/0.9327
dFC	0.0	1	0.9923/0.9963	0.8547/0.9419
dFC	0.0	2	0.9991/0.9997	0.8617/0.9413
dFC	0.0	4	0.9964/0.9966	0.8607/0.9383
dFC	0.1	1	0.9365/0.9736	0.8540/0.9392
dFC	0.1	2	0.9900/0.9983	0.8649/0.9429
dFC	0.1	4	0.9954/0.9997	0.8633/0.9425

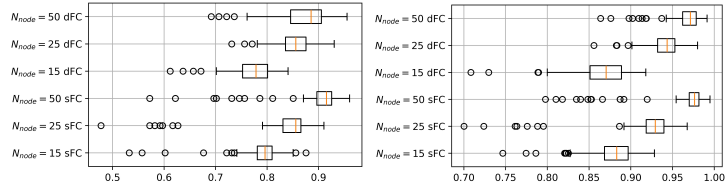
Table: Ablation study for  $N_{node} = 25$ .

## Ablation study

Data	Dropout	Channel	train ACC/AUC	test ACC/AUC
sFC	0.0	1	0.9690/0.9882	0.9003/0.9664
sFC	0.0	2	0.9986/0.9994	0.9229/0.9770
sFC	0.0	4	1.0000/1.0000	0.9245/0.9775
sFC	0.1	1	0.9199/0.9656	0.8979/0.9671
sFC	0.1	2	0.9771/0.9967	0.9165/0.9765
sFC	0.1	4	0.9920/0.9995	0.9178/0.9779
dFC	0.0	1	0.9937/0.9982	0.8726/0.9670
dFC	0.0	2	0.9995/0.9998	0.9007/0.9702
dFC	0.0	4	1.0000/1.0000	0.9089/0.9753
dFC	0.1	1	0.9493/0.9824	0.8910/0.9718
dFC	0.1	2	0.9922/0.9992	0.9032/0.9703
dFC	0.1	4	0.9979/0.9998	0.9004/0.9698

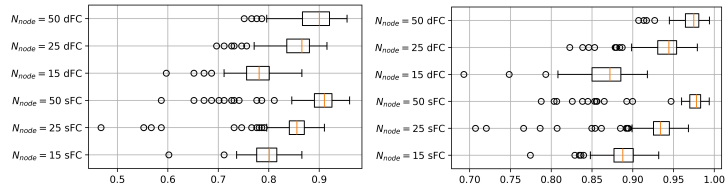
Table: Ablation study for  $N_{node} = 50$ .

# Ablation study



(a) test ACC with dropout=0.0

(b) test AUC with dropout=0.0

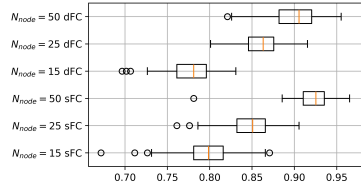


(c) test ACC with dropout=0.1

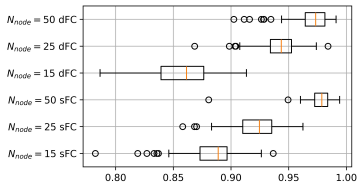
(d) test AUC with dropout=0.1

Figure: Results of CNN model with channel = 1.

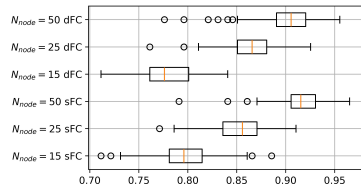
# Ablation study



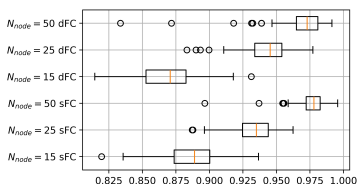
(a) test ACC with dropout=0.0



(b) test AUC with dropout=0.0



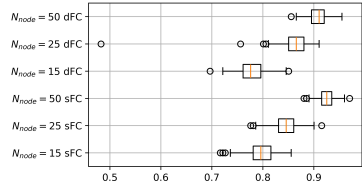
(c) test ACC with dropout=0.1



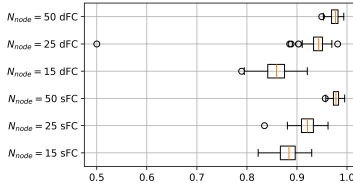
(d) test AUC with dropout=0.1

Figure: Results of CNN model with channel = 2.

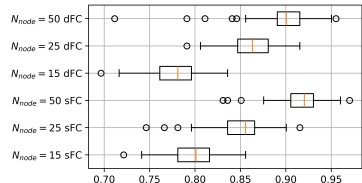
# Ablation study



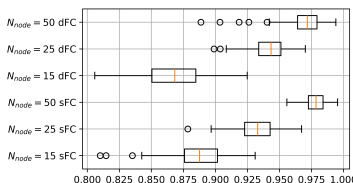
(a) test ACC with dropout=0.0



(b) test AUC with dropout=0.0



(c) test ACC with dropout=0.1



(d) test AUC with dropout=0.1

Figure: Results of CNN model with channel = 4.